Bayesian Transfer Learning with Particle Filter for Object Tracking under Asymmetric Noise Intensities

Omar Alotaibi and Brian L. Mark

***Abstract*— Using Bayesian transfer learning, we develop a particle filter approach for tracking a nonlinear dynamical motion model in a dual-sensor system where intensities of measurement noise for both sensors are asymmetric. The densities for Bayesian transfer learning are approximated with the sum of weighted particles to improve the tracking performance of the primary sensor, which experiences higher noise intensity compared to the source sensor. Simulation results are presented that validate the effectiveness of the proposed approach compared to an isolated particle filter and transfer learning applied to the unscented Kalman filter and the cubature Kalman filter.**

I. Introduction

We consider a dual-sensor system for tracking a single object, where the fields of view of the two sensors overlap. One of the sensors is referred to as the primary sensor, while the other is the source sensor. Each of the sensors employs a particle filter to track the common object along a nonlinear trajectory. We shall assume that the primary sensor's field of view (FOV) encounters higher noise intensity or clutter in its measurements compared to that of the source sensor. Our aim is to improve the tracking performance of the primary sensor by leveraging knowledge from the source sensor using Bayesian transfer learning (BTL).

Transfer learning or *knowledge transfer*, a machine learning technique, has recently been introduced into Bayesian models involving multiple tracking systems [1]. This approach is referred to as BTL [2]. Transfer learning allows knowledge gained from a source domain to improve the performance of a target domain that has challenges of performing its own task accurately. BTL has been adopted to model Gaussian process regression with multiple tasks to effectively address the interactions between the source and target tasks [3]. Additionally, online object tracking has been modeled using BTL to allow the transfer of visual priors into the tracking process framework to improve performance under complex conditions [4].

BTL has been applied to a pair of Kalman filters with asymmetric noise intensities for tracking an object following a *linear* motion model [5]. The incorporation of BTL with a Bayesian filter, referred to as a Bayesian transfer learning filter (BTLF), aims to enhance the estimation performance of the primary sensor, whose FOV is affected by severe conditions, by leveraging gained knowledge from the source sensor. BTLF has been previously applied in [6] to track a *nonlinear* motion model using a *local* approximation approach, where the posterior density follows the form of the prior density. In this approach, the predicted observation parameters, i.e., the mean and covariance, obtained from Bayesian filtering using an unscented Kalman filter, were transferred from the source sensor to the primary sensor. The BTL approach is different from measurement vector fusion (MVF) [7] and distributed estimation filtering methods such as distributed Kalman filtering (DKF) [8], [9], in which the source sensor directly transfers its estimated states or measurements to the primary sensor. The drawbacks of MVF and DKF relative to the BTLF approach are as follows: (i) higher communication overhead in transferring cluttered observation data, (ii) one time-step delay in the transferred information, and (iii) from a security or privacy perspective, the raw observation data may contain information that the source may not which to disclose.

To the best of our knowledge, there have been no previous applications of *global* approaches, whereby no explicit assumption is made about the form of the posterior density, in the context of BTLF. A popular global approach for nonlinear filtering the particle filter (PF) with importance resampling [10], [11]. Our main contribution is to approximate BTLF via a PF to track a nonlinear dynamical motion model in a dual-sensor system under asymmetric measurement noise intensities.

Our simulation results show that the estimation accuracy performance of the proposed transfer learning particle filter (TL-PF) scheme, which incorporates BTLF with PF, is significantly superior relative to the performance of an isolated PF under the same conditions. The main benefit of the proposed TL-PF approach is that it outperforms not only the isolated PF, but also the integration of unscented Kalman filter (UKF) [12] and cubature Kalman filter (CKF) [13] with BTLF, which we refer to as transfer learning unscented Kalman filter (TL-UKF) and transfer learning cubature Kalman filter (TL-CKF) respectively, as recently published in [14], [15]. This demonstrates the advantages of integrating PF with BTLF to achieve higher accuracy performances for the challenges of nonlinear motion tracking in dual-sensor systems.

The rest of the paper is organized as follows. Section II formulates the problem of tracking an object using a dual-sensor system with a nonlinear model under asymmetric measurement noise intensities. In Section III, the BTLF framework is applied to object tracking in a dual-sensor system. Section IV develops the TL-PF scheme. Numerical results are presented in Section V. The paper is concluded in Section VI.

O. Alotaibi and B.L. Mark are with the Dept. of Electrical and Computer Engineering, George Mason University Fairfax, Virginia, 22030, U.S.A. oalotaib@gmu.edu, bmark@gmu.edu

II. Dynamic System Model for Object Tracking

A. Nonlinear Motion Model

Consider a discrete-time dynamical nonlinear system [16] described in a state space representation by the following equations:

$$\mathbf{x}_k = f(\mathbf{x}_{k-1}) + \mathbf{v}_{k-1}, \tag{1}$$

$$\mathbf{z}_k = h(\mathbf{x}_k) + \mathbf{w}_k, \tag{2}$$

where $k \in \mathbb{N}_0$ denotes the time step of the discrete-time dynamical system. The state of the system at time k is represented by $\mathbf{x}_k \in \mathbb{R}^{n_\mathbf{x}}$ and $f : \mathbb{R}^{n_\mathbf{x}} \to \mathbb{R}^{n_\mathbf{x}}$ is a nonlinear state transition function. The measurement of the system observed at time k is denoted by a vector $\mathbf{z}_k \in \mathbb{R}^{n_\mathbf{z}}$, which is determined by a nonlinear function $h : \mathbb{R}^{n_\mathbf{x}} \to \mathbb{R}^{n_\mathbf{z}}$ of the state vector. The vectors $\mathbf{v}_{k-1} \in \mathbb{R}^{n_\mathbf{x}}$ and $\mathbf{w}_k \in \mathbb{R}^{n_\mathbf{z}}$ define the process and measurement noises characterizing the uncertainty in the dynamical system. The state and measurement vectors for a particular object tracking scenario are defined in Section V.

B. Dual-Sensor System with Asymmetric Noise Intensities

We consider a dual-sensor system tracking a single object following the nonlinear motion model provided in (1). The process noise of both sensors is assumed to be independent and identically distributed (i.i.d.) zero-mean Gaussian vector process, expressed as $\mathbf{v}_k \overset{\text{iid}}{\sim} \mathcal{N}(\mathbf{0}, \mathbf{Q}_\mathbf{v})$, with the same corresponding covariance $\mathbf{Q}_\mathbf{v} \in \mathbb{R}^{n_\mathbf{x} \times n_\mathbf{x}}$ for the source and the primary sensors. The two sensors each track the desired object under the same type of measurement noise, which is assumed to be Gaussian. However, the environmental and surrounding conditions according to each sensor location and its FOV are not necessarily the same. This variation in conditions leads to dissimilar measurement noise intensities that the sensors experience. As shown in Fig. 1, the source sensor measurements are denoted by $\mathbf{z}_k^\star$ with superscript $\star$ while primary sensor measurements are denoted by $\mathbf{z}_k$.

The measurement model represented in (2) will be separated for the source and primary sensors, respectively, as

$$\mathbf{z}_k^\star = h(\mathbf{x}_k) + \mathbf{w}_k^\star \text{ and } \mathbf{z}_k = h(\mathbf{x}_k) + \mathbf{w}_k, \tag{3}$$

where the measurement noise of the source and primary sensors are assumed to be i.i.d. zero-mean Gaussian, i.e., $\mathbf{w}_k^\star \overset{\text{iid}}{\sim} \mathcal{N}(\mathbf{0}, \mathbf{Q}_\mathbf{w}^\star)$ and $\mathbf{w}_k \overset{\text{iid}}{\sim} \mathcal{N}(\mathbf{0}, \mathbf{Q}_\mathbf{w})$, respectively. The measurement noise covariances are given by $\mathbf{Q}_\mathbf{w}^\star = I_\mathbf{w}^\star \mathbf{B}_\mathbf{w}$ and $\mathbf{Q}_\mathbf{w} = I_\mathbf{w} \mathbf{B}_\mathbf{w}$, where $\mathbf{B}_\mathbf{w} \in \mathbb{R}^{n_\mathbf{z} \times n_\mathbf{z}}$ is the common matrix. The noise intensities of the source, $I_\mathbf{w}^\star \in \mathbb{R}^+$, and primary, $I_\mathbf{w} \in \mathbb{R}^+$, sensors are assumed to be asymmetric, i.e., $I_\mathbf{w} > I_\mathbf{w}^\star$. The higher level of noise intensity at the primary sensor negatively impacts the reliability of its measurements and its tracking performance.

III. Bayesian Transfer Learning Filter Approach

We briefly review the BTLF framework, which was applied in [6], [14] in the context of a dual-sensor system based on the unscented Kalman filter.

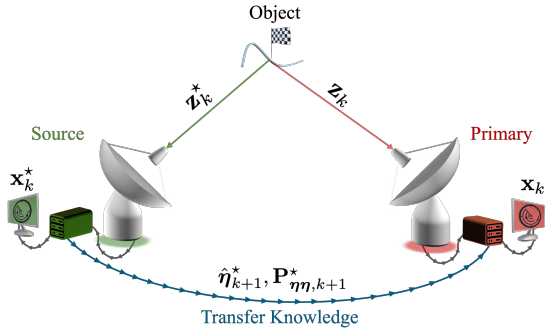

Fig. 1. Illustration of a dual-sensor system with asymmetric noise intensities integrating transfer learning technique.

A. Source Tracking Filter

In the source tracking filter, an unknown object state, denoted as $\mathbf{x}_k^\star$, of the current time step k and a predicted observation $\boldsymbol{\eta}_{k+1}^\star$ of the next time step $k+1$ are estimated given a set of observed measurements up to time step k, defined as $\mathbf{z}_{1:k}^\star = \{\mathbf{z}_1^\star, \mathbf{z}_2^\star, \ldots, \mathbf{z}_k^\star\}$. The overall posterior density of the object state and predicted observation $p(\mathbf{x}_k^\star, \boldsymbol{\eta}_{k+1}^\star \mid \mathbf{z}_{1:k}^\star)$ is estimated via two posterior densities by (see [14])

$$p(\mathbf{x}_k^\star, \boldsymbol{\eta}_{k+1}^\star \mid \mathbf{z}_{1:k}^\star) \propto p(\mathbf{x}_k^\star \mid \mathbf{z}_{1:k}^\star)\, p(\boldsymbol{\eta}_{k+1}^\star \mid \mathbf{z}_{1:k}^\star), \tag{4}$$

where the object state posterior and predicted observation densities are expressed, respectively, as

$$p(\mathbf{x}_k^\star \mid \mathbf{z}_{1:k}^\star) \propto p(\mathbf{z}_k^\star \mid \mathbf{x}_k^\star)\, p(\mathbf{x}_k^\star \mid \mathbf{x}_{k-1}^\star)\, p(\mathbf{x}_{k-1}^\star \mid \mathbf{z}_{1:k-1}^\star), \tag{5}$$

and

$$p(\boldsymbol{\eta}_{k+1}^\star \mid \mathbf{z}_{1:k}^\star) \propto p(\boldsymbol{\eta}_{k+1}^\star \mid \mathbf{x}_{k+1}^\star)\, p(\mathbf{x}_{k+1}^\star \mid \mathbf{x}_k^\star)\, p(\mathbf{x}_k^\star \mid \mathbf{z}_{1:k}^\star). \tag{6}$$

The parameter of the predicted observation density in (6) along with the predicted observations are transferred to the primary tracking filter and leveraged in the tracking filter of the next time step to improve tracking accuracy.

B. Primary Tracking Filter

The primary tracking filter receives predicted observations up to time step k from the source tracking filter. Given the set of transferred predicted observations $\boldsymbol{\eta}_{2:k}^\star$ and observed measurements up to time step k, the object state posterior density is estimated as (see [14])

$$p(\mathbf{x}_k \mid \mathbf{z}_{1:k}, \boldsymbol{\eta}_{2:k}^\star) \propto p(\mathbf{z}_k \mid \mathbf{x}_k)\; p(\boldsymbol{\eta}_k^\star \mid \mathbf{x}_k)\; p(\mathbf{x}_k \mid \mathbf{x}_{k-1}). \tag{7}$$

Via (7), the state density is estimated by incorporating transferred predicted observations from the source tracking filter as prior knowledge. This yields superior performance for the primary sensor, which has less reliable measurements.

IV. Transfer Learning for Particle Filters

We now develop a global approximation approach that integrates particle filtering with a BTLF.

A. Source Tracking Filter

The object state posterior density $p(\mathbf{x}_k^\star \mid \mathbf{z}_{1:k}^\star)$ in (5) is approximated using PF with N_s weighted particles given by

$$p(\mathbf{x}_k^\star \mid \mathbf{z}_{1:k}^\star) \approx \sum_{i=1}^{N_s} w_k^{\star(i)} \delta\left(\mathbf{x}_k^\star - \mathbf{x}_k^{\star(i)}\right), \tag{8}$$

where $\delta(\cdot)$ is the Dirac delta function. Ideally, the particles in (8) are sampled directly from the posterior density. Since sampling from the posterior density itself is not possible in most practical scenarios, weighted particles are simply drawn indirectly from a proposal density, known as the importance density, defined as

$$\mathbf{x}_k^{\star(i)} \sim q(\mathbf{x}_k^{\star(i)} \mid \mathbf{x}_{k-1}^{\star(i)}, \mathbf{z}_{1:k}^\star)\Big|_{i=1,\ldots,N_s}. \tag{9}$$

The importance density $q(\mathbf{x}_k^{\star(i)} \mid \mathbf{x}_{k-1}^{\star(i)}, \mathbf{z}_{1:k}^\star)$ is chosen to be the state transition prior $p(\mathbf{x}_k^{\star(i)} \mid \mathbf{x}_{k-1}^{\star(i)})$ given in (1). This choice of proposal density was used in [17], [18] to simplify the implementation of the PF. According to this common choice of proposal density, the computation time for sampling from the proposal importance density will be eliminated by propagating samples of the previous time step through the transition model function. After choosing the importance density as the state transition prior, the non-normalized weights in (8) and sampled particles in (9) can be obtained, respectively, as

$$w_k^{\star(i)} \propto w_{k-1}^{\star(i)}\, p(\mathbf{z}_k^\star \mid \mathbf{x}_k^{\star(i)}), \tag{10}$$

and

$$\mathbf{x}_k^{\star(i)} \sim p(\mathbf{x}_k^{\star(i)} \mid \mathbf{x}_{k-1}^{\star(i)})\Big|_{i=1,\ldots,N_s}. \tag{11}$$

Under the assumption $\mathbf{w}_k^\star \overset{\text{iid}}{\sim} \mathcal{N}(\mathbf{0}, \mathbf{Q}_\mathbf{w}^\star)$, the measurement likelihood is utilized to update non-normalized weights in (10) via

$$p(\mathbf{z}_k^\star \mid \mathbf{x}_k^{\star(i)}) = \frac{1}{(2\pi)^{n_\mathbf{z}/2}\sqrt{|\mathbf{Q}_\mathbf{w}^\star|}} \exp\left(\rho^{\star(i)}\right), \tag{12}$$

where

$$\rho^{\star(i)} = -\frac{1}{2}\left(\mathbf{z}_k^\star - h(\mathbf{x}_k^{\star(i)})\right)^T (\mathbf{Q}_\mathbf{w}^\star)^{-1}\left(\mathbf{z}_k^\star - h(\mathbf{x}_k^{\star(i)})\right), \tag{13}$$

$\mathbf{z}_k^\star \in \mathbb{R}^{n_\mathbf{z}}$ and $\mathbf{Q}_\mathbf{w}^\star$ is the covariance of the Gaussian measurement noise in (2). The updated weights in (10) are normalized to sum to one.

The resampling step reduces the effect of the degeneracy phenomenon described in [19], which appears after performing the sequential algorithm for a certain number of iterations. This phenomenon causes numerous particles, eventually a majority of particles, to receive almost zero weight, rendering them ineffective in the approximation process for the posterior density. This method measures the degeneracy at each time step by computing the effective number of particles N_{eff}, as defined in [17], and plays an important role once the effective number of particles drops below a certain threshold. The systematic resampling technique introduced in [20] is performed at every time step in the Sequential Importance Resampling (SIR) process by neglecting particles with low weights and duplicating the higher weighted particles. The new set of particles is re-weighted uniformly by assigning a new weight $w_k^{\star(i)} = 1/N_s$ to each particle as part of the SIR process.

The state posterior density, $p(\mathbf{x}_k^\star \mid \mathbf{z}_{1:k}^\star) = \mathcal{N}(\mathbf{x}_k^\star; \hat{\mathbf{x}}_k^\star, \mathbf{P}_k^\star)$, is approximately estimated based on the resampled particles and new assigned weights with mean $\hat{\mathbf{x}}_k^\star$ computed as $\hat{\mathbf{x}}_k^\star = \frac{1}{N_s}\sum_{i=1}^{N_s} \mathbf{x}_k^{\star(i)}$ and the associated covariance $\mathbf{P}_k^\star$ is obtained via

$$\mathbf{P}_k^\star = \frac{1}{N_s}\sum_{i=1}^{N_s}\left(\mathbf{x}_k^{\star(i)} - \hat{\mathbf{x}}_k^\star\right)\left(\mathbf{x}_k^{\star(i)} - \hat{\mathbf{x}}_k^\star\right)^T + \mathbf{Q}_\mathbf{v}^\star. \tag{14}$$

The predicted observation posterior density $p(\boldsymbol{\eta}_{k+1}^\star \mid \mathbf{z}_{1:k}^\star)$ in (6) is approximated similarly with a set of weighted particles via

$$p(\boldsymbol{\eta}_{k+1}^\star \mid \mathbf{z}_{1:k}^\star) \approx \sum_{i=1}^{N_s} w_{k+1}^{\star\boldsymbol{\eta}(i)} \delta\left(\boldsymbol{\eta}_{k+1}^\star - \boldsymbol{\eta}_{k+1}^{\star(i)}\right), \tag{15}$$

where the importance density $q(\boldsymbol{\eta}_{k+1}^{\star(i)} \mid \mathbf{x}_k^{\star(i)}, \mathbf{z}_{1:k}^\star)$ is chosen to be $p(\boldsymbol{\eta}_{k+1}^{\star(i)} \mid \mathbf{x}_k^{\star(i)})$ given as

$$p(\boldsymbol{\eta}_{k+1}^{\star(i)} \mid \mathbf{x}_k^{\star(i)}) = p(\boldsymbol{\eta}_{k+1}^{\star(i)} \mid \mathbf{x}_{k+1}^{\star(i)})\; p(\mathbf{x}_{k+1}^{\star(i)} \mid \mathbf{x}_k^{\star(i)}). \tag{16}$$

According to the choice of importance density in (16), particles are drawn and weighted as following:

$$\mathbf{x}_{k+1}^{\star(i)} \sim p(\mathbf{x}_{k+1}^{\star(i)} \mid \mathbf{x}_k^{\star(i)})\Big|_{i=1,\ldots,N_s}, \tag{17}$$

$$\boldsymbol{\eta}_{k+1}^{\star(i)} \sim p(\boldsymbol{\eta}_{k+1}^{\star(i)} \mid \mathbf{x}_{k+1}^{\star(i)})\Big|_{i=1,\ldots,N_s}, \tag{18}$$

and $w_{k+1}^{\star\boldsymbol{\eta}(i)} = w_k^{\star(i)} = 1/N_s$.

The mean and covariance for the predicted observation posterior density in (15), which follows a Gaussian model expressed as $p(\boldsymbol{\eta}_{k+1}^\star \mid \mathbf{z}_{1:k}^\star) = \mathcal{N}(\boldsymbol{\eta}_{k+1}^\star; \hat{\boldsymbol{\eta}}_{k+1}^\star, \mathbf{P}_{\boldsymbol{\eta}\boldsymbol{\eta},k+1}^\star)$, are estimated via uniformly weighted sampled particles and computed according to the following expressions:

$$\hat{\boldsymbol{\eta}}_{k+1}^\star = \frac{1}{N_s}\sum_{i=1}^{N_s} \boldsymbol{\eta}_{k+1}^{\star(i)}, \tag{19}$$

$$\mathbf{P}_{\boldsymbol{\eta}\boldsymbol{\eta},k+1}^\star = \frac{1}{N_s}\sum_{i=1}^{N_s}\left(\boldsymbol{\eta}_{k+1}^{\star(i)} - \hat{\boldsymbol{\eta}}_{k+1}^\star\right)\left(\boldsymbol{\eta}_{k+1}^{\star(i)} - \hat{\boldsymbol{\eta}}_{k+1}^\star\right)^T + \mathbf{Q}_\mathbf{w}^\star. \tag{20}$$

Note that the estimated mean $\hat{\boldsymbol{\eta}}_{k+1}^\star$ and covariance $\mathbf{P}_{\boldsymbol{\eta}\boldsymbol{\eta},k+1}^\star$ in (19) and (20), respectively, are transferred simultaneously to the primary tracking filter. These transferred parameters, which characterize the predicted observation density in (6), provide valuable knowledge to be leveraged in the estimation process of the primary tracking filter to enhance its tracking performance.

B. Primary Tracking Filter

The primary sensor utilizes the transferred mean and covariance of the predicted observation density from the source tracking filter as a prior to estimate the overall posterior density $p(\mathbf{x}_k \mid \mathbf{z}_{1:k}, \boldsymbol{\eta}^{\star}_{2:k})$ given in (7). Using the PF approach, the approximation of the overall posterior density via weighted particles is expressed as

$$p(\mathbf{x}_k \mid \mathbf{z}_{1:k}, \boldsymbol{\eta}^{\star}_{2:k}) \approx \sum_{i=1}^{N_s} w_k^{(i)} \delta\left(\mathbf{x}_k - \mathbf{x}_k^{(i)}\right), \tag{21}$$

where the particles in (21) are drawn from an importance density as follows:

$$\mathbf{x}_k^{(i)} \sim q(\mathbf{x}_k^{(i)} \mid \mathbf{x}_{k-1}^{(i)}, \mathbf{z}_{1:k}, \boldsymbol{\eta}^{\star}_{2:k})\Big|_{i=1,\ldots,N_s}. \tag{22}$$

By choosing the proposal density to be the state transition prior, i.e., $q(\mathbf{x}_k^{(i)} \mid \mathbf{x}_{k-1}^{(i)}, \mathbf{z}_{1:k}, \boldsymbol{\eta}^{\star}_{2:k}) = p(\mathbf{x}_k^{(i)} \mid \mathbf{x}_{k-1}^{(i)})$, the non-normalized weights in (21) are computed via

$$w_k^{(i)} \propto w_k^{\boldsymbol{\eta}(i)}\ p(\mathbf{z}_k \mid \mathbf{x}_k^{(i)}), \tag{23}$$

where the transferred predicted observation weights are denoted by $w_k^{\boldsymbol{\eta}(i)}$ and defined by

$$w_k^{\boldsymbol{\eta}(i)} \propto w_{k-1}^{(i)}\ p(\boldsymbol{\eta}^{\star}_k \mid \mathbf{x}_k^{(i)}), \tag{24}$$

and particles that approximate the overall posterior density, formulated in (22), are sampled based on the chosen proposal density as

$$\mathbf{x}_k^{(i)} \sim p(\mathbf{x}_k^{(i)} \mid \mathbf{x}_{k-1}^{(i)})\Big|_{i=1,\ldots,N_s}. \tag{25}$$

The non-normalized weights are updated using two likelihoods to incorporate the most recent observed measurement and the simultaneously transferred parameters at each time step. The transferred predicted observation weights in (24) are obtained as an initial stage for updating the overall weights in (23) by applying the transferred predicted observation likelihood $p(\boldsymbol{\eta}^{\star}_k \mid \mathbf{x}_k^{(i)})$, which is given by

$$p(\boldsymbol{\eta}^{\star}_k \mid \mathbf{x}_k^{(i)}) = \frac{1}{(2\pi)^{n_{\mathbf{z}}/2}\ \sqrt{|\mathbf{P}^{\star}_{\boldsymbol{\eta}\boldsymbol{\eta},k}|}}\ \exp\left(\rho^{\boldsymbol{\eta}(i)}\right), \tag{26}$$

where

$$\rho^{\boldsymbol{\eta}(i)} = -\frac{1}{2}\left(\hat{\boldsymbol{\eta}}^{\star}_k - h(\mathbf{x}_k^{(i)})\right)^T (\mathbf{P}^{\star}_{\boldsymbol{\eta}\boldsymbol{\eta},k})^{-1}\left(\hat{\boldsymbol{\eta}}^{\star}_k - h(\mathbf{x}_k^{(i)})\right). \tag{27}$$

After updating the weights through the transferred predicted observation likelihood, the measurement likelihood $p(\mathbf{z}_k \mid \mathbf{x}_k^{(i)})$ is employed to compute the weights in (23). The measurement likelihood is given by

$$p(\mathbf{z}_k \mid \mathbf{x}_k^{(i)}) = \frac{1}{(2\pi)^{n_{\mathbf{z}}/2}\ \sqrt{|\mathbf{Q}_{\mathbf{w}}|}}\ \exp\left(\rho^{(i)}\right), \tag{28}$$

where

$$\rho^{(i)} = -\frac{1}{2}\left(\mathbf{z}_k - h(\mathbf{x}_k^{(i)})\right)^T (\mathbf{Q}_{\mathbf{w}})^{-1}\left(\mathbf{z}_k - h(\mathbf{x}_k^{(i)})\right). \tag{29}$$

The above likelihoods, expressed in (26) and (28), are formulated under the assumption of the measurement model given by (2). Unlike the isolated PF algorithm, the particle weights in the TL-PF are updated in (24) by leveraging the transferred density parameters, characterized by the mean $\hat{\boldsymbol{\eta}}^{\star}_k$ and its associated covariance $\mathbf{P}^{\star}_{\boldsymbol{\eta}\boldsymbol{\eta},k}$, which are estimated at the previous time step $k-1$ from the source tracking filter as an additive step introduced mainly for incorporating transferred parameters within the process of the PF framework in addition to the updating step in (28) and (29) via newly observed measurement $\mathbf{z}_k$ with its covariance $\mathbf{Q}_{\mathbf{w}}$. The overall weights associated with each individual particle in (23) are normalized to sum to one.

Similar to the source tracking filter, drawn particles along with their normalized weights are resampled using the systematic resampling technique to mitigate the degeneracy phenomenon effect where the resultant weights are identically equal to $1/N_s$. The overall state posterior density in (21) is modeled as a Gaussian density, expressed as $p(\mathbf{x}_k \mid \mathbf{z}_{1:k}, \boldsymbol{\eta}^{\star}_{2:k}) = \mathcal{N}(\mathbf{x}_k; \hat{\mathbf{x}}_k, \mathbf{P}_k)$. The mean $\hat{\mathbf{x}}_k$ and associated covariance $\mathbf{P}_k$ of this posterior density are estimated using N_s resampled particles as follows:

$$\hat{\mathbf{x}}_k = \frac{1}{N_s}\sum_{i=1}^{N_s} \mathbf{x}_k^{(i)}, \tag{30}$$

$$\mathbf{P}_k = \frac{1}{N_s}\sum_{i=1}^{N_s}\left(\mathbf{x}_k^{(i)} - \hat{\mathbf{x}}_k\right)\left(\mathbf{x}_k^{(i)} - \hat{\mathbf{x}}_k\right)^T + \mathbf{Q}_{\mathbf{v}}. \tag{31}$$

V. Simulation Results

A. Tracking System Model and Parameters Settings

For our simulations, we consider a single maneuvering object with an unknown state vector to be tracked by a dual-sensor system. We adopt the nonlinear motion model in [21] given by

$$\mathbf{x}_k = \begin{bmatrix} 1 & \frac{\sin(\Omega_{k-1}T_s)}{\Omega_{k-1}} & 0 & -\left(\frac{1-\cos(\Omega_{k-1}T_s)}{\Omega_{k-1}}\right) & 0 \\ 0 & \cos(\Omega_{k-1}T_s) & 0 & -\sin(\Omega_{k-1}T_s) & 0 \\ 0 & \frac{1-\cos(\Omega_{k-1}T_s)}{\Omega_{k-1}} & 1 & \frac{\sin(\Omega_{k-1}T_s)}{\Omega_{k-1}} & 0 \\ 0 & \sin(\Omega_{k-1}T_s) & 0 & \cos(\Omega_{k-1}T_s) & 0 \\ 0 & 0 & 0 & 0 & 1 \end{bmatrix} \mathbf{x}_{k-1} + \mathbf{v}_{k-1}. \tag{32}$$

The object state is given by $\mathbf{x}_k = [x_k, \dot{x}_k, y_k, \dot{y}_k, \Omega_k]^T$, which consists of the Cartesian coordinates of the object's position (x_k, y_k), the object's velocity $(\dot{x}_k, \dot{y}_k)$, and the turn rate Ω_k. The process noise $\mathbf{v}_k \overset{\text{iid}}{\sim} \mathcal{N}(0, \mathbf{Q}_{\mathbf{v}})$ with associated covariance

$$\mathbf{Q}_{\mathbf{v}} = \begin{bmatrix} q_1\frac{T_s^4}{4} & q_1\frac{T_s^3}{2} & 0 & 0 & 0 \\ q_1\frac{T_s^3}{2} & q_1T_s^2 & 0 & 0 & 0 \\ 0 & 0 & q_1\frac{T_s^4}{4} & q_1\frac{T_s^3}{2} & 0 \\ 0 & 0 & q_1\frac{T_s^3}{2} & q_1T_s^2 & 0 \\ 0 & 0 & 0 & 0 & q_2T_s \end{bmatrix}. \tag{33}$$

As in Section II-B, the error process noise covariances of the source and primary tracking filters are assumed to be identical.

The dual-sensor system observes measurements that follow the nonlinear measurement models in (3) with asymmetric measurement noise intensities for the source and primary tracking filters. The measurement vector for each sensor comprises the object's range, $r_k = \sqrt{x_k^2 + y_k^2}$, and bearing angle, $\zeta_k = \arctan(y_k/x_k)$, i.e., $\mathbf{z}_k = [r_k, \zeta_k]^T$. The measurement noises of the source and primary tracking filters are zero-mean Gaussian processes denoted as $\mathbf{w}_k^\star \overset{\text{iid}}{\sim} \mathcal{N}(\mathbf{0}, \mathbf{Q}_\mathbf{w}^\star)$ and $\mathbf{w}_k \overset{\text{iid}}{\sim} \mathcal{N}(\mathbf{0}, \mathbf{Q}_\mathbf{w})$, with associated covariances $\mathbf{Q}_\mathbf{w}^\star = I_\mathbf{w}^\star \, \mathbf{B}_\mathbf{w}$ and $\mathbf{Q}_\mathbf{w} = I_\mathbf{w} \, \mathbf{B}_\mathbf{w}$, respectively, where $\mathbf{B}_\mathbf{w} = \text{diag}[\sigma_r^2, \sigma_\zeta^2]$. The noise intensity levels $I_\mathbf{w}^\star$ and $I_\mathbf{w}$ represent conditions impacting the individual sensors.

TABLE I
SIMULATION PARAMETER SETTINGS

Parameter	Value	Parameter	Value
$n_\mathbf{x}$	5	$n_\mathbf{z}$	2
T_s	1 s	MC runs	$10,000$
q_1	0.1 m^2/s^4	q_2	1.75×10^{-2} rad^2/s^3
σ_r	10 m	σ_ζ	$\sqrt{10} \times 10^{-3}$ rad
$I_\mathbf{w}^\star$	1	$I_\mathbf{w}$	$1 \rightarrow 8$

The simulation parameter settings for the dual-sensor tracking system are specified in Table I. The object maneuvers in a two-dimensional trajectory with a duration of 100 time steps as shown in Fig.2. The object's state and covariance are initialized as $\mathbf{x}_0 = [1000 \text{ m}, 300 \text{ m/s}, 1000 \text{ m}, 0 \text{ m/s}, -3^\circ/\text{s}]^T$ and $\mathbf{P}_0 = \text{diag}[100 \text{ m}^2, 10 \text{ m}^2/\text{s}^2, 100 \text{ m}^2, 10 \text{ m}^2/\text{s}^2, 100 \times 10^{-3} \text{ rad}^2/\text{s}^2]$. The root-mean square error (RMSE) performance results are evaluated by averaging $10,000$ Monte Carlo (MC) simulation runs. The object trajectory and parameters settings are identical to the simulation realization in [6], [14] to present a fair comparison with the previous results obtained from incorporating BTLF into the UKF and CKF local approximation approaches.

B. Performance Evaluation

We evaluate the proposed TL-PF using the tracking scenario in Fig. 2. The performance of the proposed TL-PF and isolated PF are evaluated in terms of RMSE per time step, as shown in Fig. 3. For comparison with the results in [14], the figure also shows the RMSE performance of the isolated UKF and isolated third-degree CKF, as well as that of the transfer learning versions of the UKF and CKF, denoted as TL-UKF and TL-CKF, respectively. The proposed TL-PF algorithm with $N_s = 6000$ particles (blue dashed line with + marks) achieves RMSE values of 7.85 m and 14.38 m at time steps $k = 48$ s and $k = 75$ s, respectively, under the noise intensities of $I_\mathbf{w} = 4$ (primary sensor) and $I_\mathbf{w}^\star = 1$ (source sensor). In comparison, the isolated version of PF

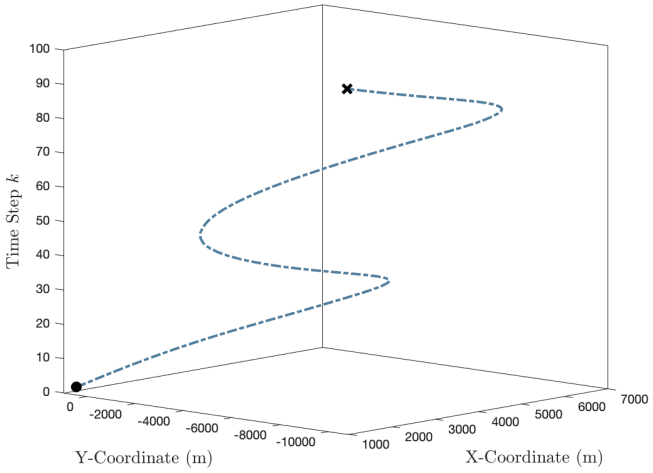

Fig. 2. Trajectory of object maneuvering in two-dimensions of Cartesian coordinates beside time step, where ● and ✖ indicate the initial and end points, respectively.

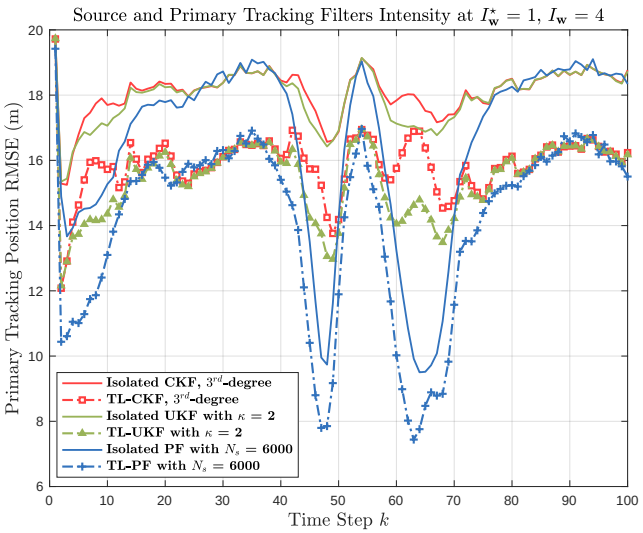

Fig. 3. A comparison of obtained RMSE performance plots versus time step for the proposed algorithm TL-PF (blue dashed line with + marks), TL-UKF [14], TL-CKF [14], and isolated filters.

(blue solid line) has RMSE values of 9.73 m and 17.34 m at the same noise level and time steps. Furthermore, the proposed TL-PF algorithm (with $N_s = 6000$) achieves an RMSE of 13.10 m at time step $k = 10$ s, outperforming the third-degree TL-CKF and TL-UKF (with $\kappa = 2$), which obtain RMSE values of 15.72 m and 14.35 m, respectively, under the same conditions. From Fig. 3, we see that the performance of the proposed TL-PF is always superior to that of the isolated approaches. For most of the trajectory, TL-PF performs significantly better than TL-CKF and TL-UKF. In the intervals of $(20, 40)$ s and $(85, 95)$ s, TL-PF performs comparably to TL-CKF and TL-UKF. We note, however, that the performance of TL-PF can be further improved by increasing the number of particles, N_s, at the expense of higher computational cost.

To further demonstrate the behavior of the proposed TL-

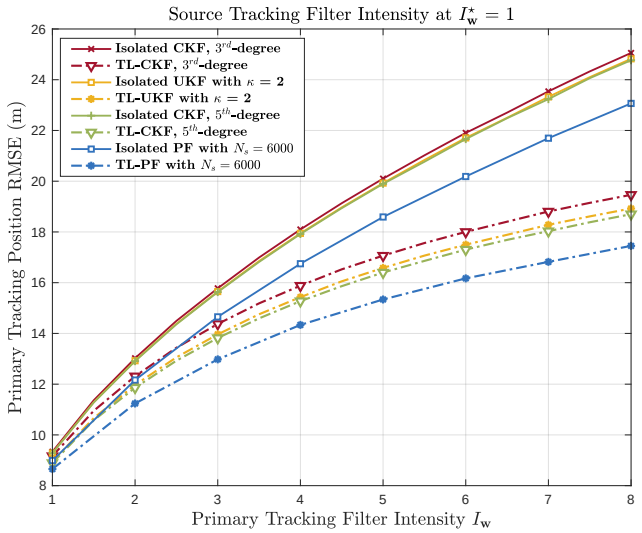

Fig. 4. The overall RMSE performance of the proposed TL-PF algorithm (with $N_s = 6000$) under varying primary noise intensity $I_{\mathbf{w}}$, plotted alongside the performance of local BTLF approaches in [14].

PF algorithm, we evaluate its overall RMSE performance, averaged over 100 time steps and $10,000$ MC iterations, under various levels of primary noise intensity $I_{\mathbf{w}}$, while fixing the intensity level of source noise $I_{\mathbf{w}}^{\star}$. As shown in Fig. 4, the accuracy gain of the TL-PF (blue dashed line marked with $*$) compared to the isolated traditional PF increases as the level of primary noise intensity $I_{\mathbf{w}}$ increases. For instance, under $I_{\mathbf{w}} = 4$, the TL-PF (with $N_s = 6000$) achieves an RMSE value of 14.33 m, while the isolated PF has an RMSE of 16.74 m with a reduction in estimation error of approximately 2.41 m. Similarly, under $I_{\mathbf{w}} = 8$, the TL-PF has an RMSE of 17.45 m compared to 23.06 m for the isolated PF with a reduction of 5.61 m. Furthermore, the TL-PF (with $N_s = 6000$) outperforms the fifth-degree TL-CKF (green dashed line with $\triangledown$ marks) and is capable of achieving an accuracy gain value of approximately 1.24 m under a level of primary noise intensity $I_{\mathbf{w}} = 8$.

VI. Conclusion

We developed a BTL approach for particle filtering, TL-PF, in a dual-sensor system with asymmetric measurement noise intensities at the primary and source sensors. By leveraging predicted measurement information transferred from the source sensor, the primary sensor, which experiences the higher noise intensity, is able to achieve a significant gain in tracking performance compared to an isolated particle filter, with no applying of transfer learning. We also compared the performance of the proposed transfer learning particle filter schemes to earlier schemes based on applying Bayesian transfer learning to the unscented Kalman filter and the cubature Kalman filter, referred to as TL-UKF and TL-CKF, respectively.

References

[1] S. J. Pan and Q. Yang, "A survey on transfer learning," *IEEE Trans. Knowl. Data Eng.*, vol. 22, no. 10, pp. 1345–1359, 2009.

[2] A. Karbalayghareh, X. Qian, and E. R. Dougherty, "Optimal Bayesian transfer learning," *IEEE Trans. Signal Process.*, vol. 66, no. 14, pp. 3724–3739, 2018.

[3] ——, "Optimal Bayesian transfer regression," *IEEE Signal Process. Lett.*, vol. 25, no. 11, pp. 1655–1659, 2018.

[4] Q. Wang, F. Chen, J. Yang, W. Xu, and M.-H. Yang, "Transferring visual prior for online object tracking," *IEEE Trans. Image Process.*, vol. 21, no. 7, pp. 3296–3305, 2012.

[5] C. Foley and A. Quinn, "Fully probabilistic design for knowledge transfer in a pair of Kalman filters," *IEEE Signal Process. Lett.*, vol. 25, no. 4, pp. 487–490, 2017.

[6] O. Alotaibi and B. L. Mark, "Object tracking incorporating transfer learning into an unscented Kalman filter," in *Proc. 58th Annu. Conf. Inf. Sci. Syst. (CISS)*, Princeton, NJ, March 2024, pp. 1–6.

[7] D. Willner, C. B. Chang, and K. P. Dunn, "Kalman filter algorithms for a multi-sensor system," in *Proc. IEEE Conf. Decis. Control Including 15th Symp. Adapt. Processes*, 1976, pp. 570–574.

[8] R. Olfati-Saber, "Distributed Kalman filtering for sensor networks," in *Proc. 46th IEEE Conf. Decis. Control*, 2007, pp. 5492–5498.

[9] S. P. Talebi and S. Werner, "Distributed Kalman filtering: Consensus, diffusion, and mixed," in *Proc. IEEE Conf. Control Technol. Appl.*, 2018, pp. 1126–1132.

[10] N. J. Gordon, D. J. Salmond, and A. F. M. Smith, "Novel approach to nonlinear/non-Gaussian Bayesian state estimation," *Proc. Inst. Elect. Eng. F*, vol. 140, no. 2, pp. 107–113, April 1993.

[11] F. Gustafsson, F. Gunnarsson, N. Bergman, U. Forssell, J. Jansson, R. Karlsson, and P.-J. Nordlund, "Particle filters for positioning, navigation, and tracking," *IEEE Trans. Signal Process.*, vol. 50, no. 2, pp. 425–437, 2002.

[12] S. Julier, J. Uhlmann, and H. F. Durrant-Whyte, "A new method for the nonlinear transformation of means and covariances in filters and estimators," *IEEE Trans. Autom. Control*, vol. 45, no. 3, pp. 477–482, March 2000.

[13] I. Arasaratnam and S. Haykin, "Cubature Kalman filters," *IEEE Trans. Autom. Control*, vol. 54, no. 6, pp. 1254–1269, 2009.

[14] O. Alotaibi and B. L. Mark, "Object tracking incorporating transfer learning into unscented and cubature Kalman filters," *arXiv:2408.07157*, 2024.

[15] ——, "Incorporating multi-source transfer learning into an unscented Kalman filter for object tracking," in *Proc. 59th Annu. Conf. Inf. Sci. Syst. (CISS)*, Baltimore, MD, March 2025, pp. 1–6.

[16] Y. Ho and R. Lee, "A Bayesian approach to problems in stochastic estimation and control," *IEEE Trans. Autom. Control*, vol. 9, no. 4, pp. 333–339, October 1964.

[17] J. S. Liu and R. Chen, "Sequential Monte Carlo methods for dynamic systems," *J. Amer. Statist. Assoc.*, vol. 93, no. 443, pp. 1032–1044, 1998.

[18] M. S. Arulampalam, S. Maskell, N. Gordon, and T. Clapp, "A tutorial on particle filters for online nonlinear/non-Gaussian Bayesian tracking," *IEEE Trans. Signal Process.*, vol. 50, no. 2, pp. 174–188, Feb. 2002.

[19] A. Doucet, S. Godsill, and C. Andrieu, "On sequential Monte Carlo sampling methods for Bayesian filtering," *Statist. Comput.*, vol. 10, no. 3, pp. 197–208, Jul. 2000.

[20] G. Kitagawa, "Monte Carlo filter and smoother for non-Gaussian nonlinear state space models," *J. Comput. Graph. Statist.*, vol. 5, no. 1, pp. 1–25, 1996.

[21] Y. Bar-Shalom, X. R. Li, and T. Kirubarajan, *Estimation with Applications to Tracking and Navigation: Theory Algorithms and Software*. New York, NY: Wiley, 2001.